Biochimie 162 (2019) 156–166

Contents lists available at ScienceDirect

Biochimie

journal homepage: www.elsevier.com/locate/biochi

Research paper

A large-scale comparative analysis of affinity, thermodynamics and functional characteristics of interactions of twelve cytochrome P450 isoforms and their redox partners

Evgeniy O. Yablokov [a, *, 1], Tatsiana A. Sushko [b, c, 1], Pavel V. Ershov [a], Anna V. Florinskaya [a], Oksana V. Gnedenko [a], Tatsiana V. Shkel [b], Irina P. Grabovec [b], Natallia V. Strushkevich [b], Leonid A. Kaluzhskiy [a], Sergey A. Usanov [b], Andrei A. Gilep [a, b], Alexis S. Ivanov [a]

[a] Federal State Budgetary Institution "V.N. Orekhovich Research Institute of Biomedical Chemistry", 119121, Moscow, Pogodinskaya str. 10, building 8, Russia
[b] Institute of Bioorganic Chemistry National Academy of Science of Belarus, 220141, Minsk, Kuprevicha str. 5/2, Republic of Belarus
[c] Department of Bioengineering, School of Engineering, The University of Tokyo, 4-6 – 1 Shirokanedai, Minato-ku, 108-8639, Tokyo, Japan

ARTICLE INFO

Article history:
Received 16 January 2019
Accepted 24 April 2019
Available online 26 April 2019

Keywords:
Cytochrome P450
Cytochrome P450 reductase
Adrenodoxin
Optical biosensor
Thermodynamics
Protein-protein interactions

ABSTRACT

The aim of the present work was to establish the thermodynamic and functional differences in the protein-protein interactions between the components of the P450-dependent mitochondrial (mit) and microsomal (mic) monooxygenase systems using 12 different isoforms of cytochromes P450 and two redox partners, NADPH-dependent cytochrome P450 reductase (CPR) and adrenodoxin (Adx). Comparative analysis of the affinity, thermodynamics, enzymatic activity and the ability for one-electron reduction has been carried out. The study of protein-protein interactions to determine the equilibrium dissociation constants (Kd) was performed using surface plasmon resonance (SPR) biosensor Biacore 3000. We demonstrated that CPR and Adx interacted with both, micCYPs and mitCYPs, with different affinities (Kd values ranged from 0.01 to 2 μM). All complexes of microsomal (micCYP) and mitochondrial (mitCYP) cytochrome P450 with redox partners can be divided into three groups depending on the prevalent role of either enthalpy or entropy contribution. About 90% of CYP/redox partner complexes were entropy-driven, while the contribution of enthalpy and entropy differed significantly in case of mitCYP/Adx complexes. The CYP11A1/Adx complex was enthalpy-driven, while CYP11B1/Adx and CYP11B2/Adx complexes were entropy-driven. Thermodynamic discrimination of mitCYPs/Adx complexes is likely associated with the different functional impact of CYP11A1 and CYP11B. The exception was the enthalpy-entropy-driven (mixed type) CYP21A2/Adx complex. CPR and Adx were able to transfer the first electron to micCYPs while mitCYPs demonstrated high specificity to Adx. Productive catalysis for mitCYPs observed only in the presence of Adx/AdR pair, while in case of steroidogenic micCYPs (CYP17A1, CYP19A1, and CYP21A2) it was found either in the presence of a CPR or an Adx/AdR pair. From the evolutionary point of view, the type 1 electron transport system (mitCYPs, Adx and NADPH-dependent adrenodoxin reductase (AdR)) increased the specialization of protein-protein interactions (PPI) significantly, which was accompanied by an increase in the specificity of electron transfer. In contrast, the evolution of the type 2 electron transport system (micCYPs and CPR) led to an increase in versatility of PPI as demonstrated for steroidogenic microsomal cytochrome P450s. Our data enhance the current understanding of molecular recognition and summarize qualitative and thermodynamic characteristics of protein-protein interactions in the P450-dependent mitochondrial and microsomal monooxygenase systems.

Abbreviations: CYP, Cytochrome P450; mitCYP, mitochondrial CYPs; micCYP, microsomal CYPs; RP, redox partners; ETS, electron transfer systems (ETS-1 - Class I ETS, ETS-2 - Class II ETS, ETS-10 - Class X ETS); Adx, adrenodoxin; AdR, FAD-containing adrenodoxin reductase; CPR, NADPH- dependent cytochrome P450 reductase; PPI, protein-protein interactions; SPR, Surface Plasmon Resonance; RU, the resonant units; Kd, equilibrium dissociation constants; enthalpy and entropy, ΔG, ΔH, ΔS - changes of the Gibbs free energy; HEPES, 4-(2-hydroxyethyl)-1-piperazineethanesulfonic acid; EDC, 1-ethyl-3-(3-dimethylaminopropyl)-carbodiimide-HCl; NHS, N-hydroxysuccinimide.

* Corresponding author. Department of Proteomics & Mass-spectrometry, Federal State Budgetary Institution "V.N. Orekhovich Research Institute of Biomedical Chemistry", Russia.
E-mail address: evgeyablokov1988@mail.ru (E.O. Yablokov).
[1] These authors contributed equally to the work described in this manuscript.

https://doi.org/10.1016/j.biochi.2019.04.020
0300-9084/

1. Introduction

Cytochrome P450s (**CYP**s) are a large superfamily of monooxygenases that being found in all domains of living systems including prokaryotes and eukaryotes. Mammalian CYPs are membrane-bound proteins; the human genome contains 57 genes encoding different CYP isozymes [1]. They are found in all tissues and responsible for a variety of physiological processes. CYPs participate in the metabolism of a wide range of endogenous and exogenous substrates, including biotransformation of drugs and toxins, biosynthesis and catabolism of cholesterol, vitamin D3, steroid hormones, bile acids, and prostaglandins. The most common CYP reaction is monooxygenation where one atom of molecular oxygen is activated by two electrons supplied by NADPH (NADH), while the other one is reduced to the water molecule [2,3]. CYP acquires electrons from [2Fe–2S] protein adrenodoxin (**Adx**), which receives them from NADPH through FAD-containing adrenodoxin reductase (**AdR**) [4] or NADPH-dependent cytochrome P450 reductase (**CPR**) containing FAD- and FMN-domains [5,6]. The study of affinity and thermodynamics of protein-protein interactions (PPI) in the P450-dependent monooxygenases is of fundamental importance for a better understanding of structural and functional relationships between the components of this system and identification of the discrimination of enthalpy and entropy contributions to complex formation [7–9]. This work was aimed at establishing the thermodynamic and functional differences in protein-protein interactions between the components of the P450-dependent mitochondrial and microsomal monooxygenase systems using twelve different isoforms of cytochrome P450s and two redox partners CPR and Adx. It's worth mentioning that current study was a continuation of our previous research on characterization of the affinity and thermodynamics of molecular complexes formed by nine different isoforms of mammalian CYPs and two isoforms of human cytochrome b5 (**CYB5**) using a surface plasmon resonance (SPR) optical biosensor [10]. In the present study we carried out SPR experiments under similar experimental conditions but using broader spectrum of CYP/RP complexes studied, so it gave the possibility of comparing the kinetic, equilibrium and thermodynamic parameters obtained. Application of SPR biosensors for the analysis of protein-protein interactions was demonstrated in previous studies [11–13] and discussed in reviews [14–16]. In particular, SPR has been shown useful for monitoring the protein-protein interactions in the P450-dependent systems [17]. Earlier studies with CYPs reported that this technology can be used to calculate ligand binding parameters [18] and is effective in measuring the interactions between CYPs and redox partners [19–22].

Here, for the first time, we apply the SPR technology to identify the affinity and thermodynamic parameters of 24 protein-protein interactions (PPI) between three mitochondrial cytochromes P450 (mitCYP) and nine microsomal CYPs (micCYP) and their redox partners - CPR and Adx. The functional significance of PPIs was characterized by a single-electron reduction method and enzyme activity assays. The equilibrium dissociation constants (Kd) of the complexes as well as the changes in the Gibbs free energy (ΔG), enthalpy (ΔH) and entropy (-TΔS) were calculated for 24 pairs of proteins (CYP/CPR and CYP/Adx) in total.

2. Materials and methods

2.1. Equipment

Real-time measurements of PPIs were performed on a Biacore 3000 SPR biosensor (GE Healthcare, USA) in a temperature range from 10 to 40 °C using CM5 optical chips coated with a layer of carboxymethylated dextran. The sensorgrams of PPIs were registered as a continuous record of the biosensor signal changes expressed in resonance units, RU. 1 RU is approximately equal to the binding of 1 pg of protein per 1 mm^2 of the chip surface. Proteins purification procedures were performed using the chromatographic system Akta Purifier (GE Healthcare, USA). Spectrophotometric measurements were performed using Shimadzu UV-3000 spectrophotometer (Shimadzu, Japan) and Cary UV–Vis–NIR (Agilent, USA).

Analysis of the product of reactions catalyzed by mic- and mitCYPs was carried out using HPLC Hewlett Packard HP 1090 series II/L (Hewlett Packard, USA) equipped with C18-column μ-Bondapak (3.9 × 300 mm) and a diode array detector or Agilent 1200 Series L equipped with chromatography column Eclipse Plus C18 (4.6 × 250 mm, particle size 5 μm) and a diode array detector (Agilent, USA).

2.2. Chemicals

The following reagents were used: progesterone, 11-deoxycorticosterone, testosterone, lanosterol, 7-dehydrocholesterol, diclofenac, cymal-5, CHAPS, NADPH, HEPES, Tris, DLPC, EDTA (Sigma-Aldrich, USA); Ni-NTA-Agarose (Qiagen, USA); Emulgen 913 (Kao Atlas, Japan); dithiothreitol (Gibco BRL, USA). Restrictases and DNA modifying enzymes were purchased from New England Biolabs and Promega, USA.

Special reagents for biosensor measurements were obtained from GE Healthcare (GE Healthcare, USA): HBS-EP + buffer (150 mM NaCl, 10 mM HEPES, 3 mM EDTA, 0.05% P-20 surfactant, pH 7.4), HBS-N buffer (150 mM NaCl, 10 mM HEPES, pH 7.4), 50 mM NaOH solution, 70% glycerol solution, 10 mM acetate buffer (pH 4.5), the amino-coupling kit for covalent immobilization of proteins on the CM5 optical chip: 1-ethyl-3- (3-dimethylaminopropyl) carbodiimide-HCl (EDC), N-hydroxysuccinimide (NHS), 1 M ethanolamine-HCl (pH 8.5). Other reagents of analytical purity were obtained from local suppliers.

2.3. Proteins

In the current study, 12 recombinant highly purified (>95% by SDS-PAGE) mammalian CYPs isoforms were used (human CYP2C9, CYP21A2, CYP19A1, CYP1B1, CYP2C19, CYP51A1, CYP3A4, CYP3A5; horse CYP17A1; bovine CYP11A1 and human CYP11B1, CYP11B2), as well as CPR, Adx and AdR. The methods for purification and functional activity assays of recombinant CYPs have been described previously: CYP3A4 and CYP3A5 [23], CYP17A1 [24], CYP51A1 [25], CYP11A1 [26], CYP11B1 and CYP11B2 [27], CYP2C9 [28]. CYP1B1 was purified according to Refs. [23–28]. Recombinant Adx, AdR, CPR were purified as described earlier [23,29,30]. Human CYP5A1 [31] and hemoglobin were used as a negative control for specificity of PPIs. Human hemoglobin was isolated from lysed red blood cells and purified by anion-exchange chromatography as described in Ref. [32].

2.4. One-electron reduction of CYPs

In order to find out if transfer of the first electron from NADPH to the mit/micP450 heme iron is possible, electron transport was analyzed using P450 redox system containing CPR or Adx and different CYPs. One-electron reduction of CYPs was performed at 25 °C in 50 mM Tris-HCl buffer, pH 7.4 containing CYP: AdR: Adx at

a molar ratio of 1:0.5:2 respectively in the case of mitochondrial electron donors or CYP: CPR at a molar ratio 1:2 respectively in the case of microsomal electron donors. Mixture was saturated with CO by extensive bubbling with the gas in a quartz cuvette. NADPH was added to the final concentration 250 μM. The reduced form of CYPs was detected as a peak at 450 nm by recording a characteristic CO-difference spectrum. Spectra (250–800 nm) were recorded regularly until no further change was detected. The kinetics of complex formation were determined by plotting extent of the reduced complex formation against reaction time and fitting the resultant data using Origin software. To control the efficiency of the first electron transfer, sodium dithionite was used for chemical reduction [33]. Reaction conditions were the same as described above, sodium dithionite has been added to final concentration 1 mg/ml instead of NADPH. The amount of reduced form of CYPs was detected as a peak at 450 nm. Efficiency of enzymatic reduction was estimated as a percentage of chemical reduction with sodium dithionite.

2.5. Estimation of CYPs enzymatic activity

Enzymatic activity of CYPs with microsomal electron donors was measured in the reconstituted system as described previously [25–28,34–37]. Briefly, aliquots of concentrated recombinant proteins (0.5 μM micCYP and 1 μM CPR or 0.5 μM mitCYP, 0.5 μM Adx and 0.25 μM AdR) were mixed and preincubated for 5 min at room temperature. Substrates diluted in ethanol (testosterone for CYP3A4 and CYP3A5, lanosterol for CYP51A1, 7-dehydrocholesterol for CYP11A1, diclofenac for CYP2C9, omeprazole for CYP2C19, progesterone for CYP17A1, CYP1B1 and CYP21A1, androstenedione for CYP19A1, 11-deoxycortisol for CYP11B1, CYP11B2) were added to the reaction mixture at a final concentration of 100 μM. After preincubation at 37 °C for 10 min, the reaction was started by adding NADPH at a final concentration of 0.25 mM. Aliquots (0.5 ml) were taken from incubation mixture at chosen time intervals. Reaction was stopped by addition of 5 ml of methylene chloride, vortex mixed, and then centrifuged at 10,000 rpm for 10 min. The organic layer was carefully removed and dried under argon flow. Hundred microliters of methanol was added to the pellet and steroids were analyzed. The concentrations of the metabolites were measured by HPLC and UV detection methods.

2.6. Immobilization of CPR and Adx on the CM5 optical chip

The CPR and Adx were covalently immobilized on the surface of the CM5 chip according to the standard amino-coupling protocol. The carboxyl groups of dextran were activated by injecting a mixture of 0.4 M EDC and 0.1 M NHS for 7 min at a flow rate of 5 μl/min. The protein sample diluted to 15 μg/ml in 10 mM sodium acetate (pH 4.5) was injected for 10 min at a flow rate of 2 μl/min. Finally, ethanolamine-HCl (1.0 M) solution was injected for 1 min at a flow rate of 5 μl/min to block the unreacted carboxyl groups of dextran. The amount of CPR and Adx immobilized on the chip surface were approximately 100 fmol and 150 fmol, respectively.

2.7. SPR analysis of PPIs between CYPs and immobilized CPR and Adx

The interactions of twelve different CYP isoforms with immobilized CPR and Adx were measured in a concentration range from 10 to 5000 nM (CYP samples were diluted with HBS-EP + buffer) and in the temperature range from 10 to 40 °C. The analyzed CYP was injected through the control (without immobilized proteins) and working channels of the optical biosensor for 7 min at a flow rate of 5 μl/min. To check the specificity of PPI, hemoglobin (50 μM) and CYP5A1 (10 μM) were injected for 7 min at a flow rate of 5 μl/min too.

The resulting sensorgrams were obtained by subtracting the control channel signals from the working channel ones. Regeneration of the optical chip surface was performed after each protein injection using a buffer containing 10 mM HEPES (pH 7.4), 1 M NaCl and 0.2% CHAPS for 1 min at a flow rate of 50 μl/min. The data were fitted using Biacore BIAevaluation software v. 4.1 (GE Healthcare, USA) to obtain the association and dissociation rate constants (k_{on} and k_{off}, respectively) as well as the equilibrium dissociation constant of the complexes (Kd).

The Gibbs free energy (ΔG) was calculated from the equation using the Kd value obtained.

$$\Delta G = RT \ln Kd \quad (1)$$

where T is the absolute temperature (K), R - universal gas constant (kcal·mol^{-1}·K^{-1}), Kd - equilibrium dissociation constant of the protein-protein complex (M).

Enthalpy change (ΔH) was determined by plotting lnKd versus 1000/T according to the equation

$$InKd = \left(\frac{\Delta H}{R}\right) * \left(\frac{1000}{T}\right) - \left(\frac{\Delta S}{R}\right) \quad (2)$$

using the slope of the linear regression line (ΔH/R).

The entropy change (ΔS) was calculated from the van't Hoff equation

$$\Delta G = \Delta H - T\Delta S \quad (3)$$

3. Results

3.1. Affinity and functional characterization of CYP/RP interactions by SPR

Affinity characterization of complex formation between twelve CYPs with CPR and Adx is presented in Table 1, and some typical examples of SPR sensorgrams are shown in Fig. 1. The data in Table 1 demonstrate that CPR and Adx interact with both, micCYPs and mitCYPs, with different affinities. CYP5A1 (or thromboxane synthase) used as a negative control did not interact with any redox partners. From the one hand, it is to be noted that the affinity of micCYPs 2C19, 19A1, 17A1, 3A4, and mitCYPs 11A1, 11B1, 11B2 was 4–30 times higher toward Adx compared with CPR. From the other hand, the Kd value of CYP2C9/CPR was 7 times lower than CYP2C9/Adx. The study of CYP-containing systems requires a combination of methods that enable both to evaluate the interactions between CYPs and their RP and to give insight into functional characteristics of these interactions. For this purpose, we carried out two functional activity tests of CYPs (Table 1). To activate molecular oxygen, CYP requires two electrons provided by RP. When transferring the first electron, the heme iron is reduced, and the complex with oxygen (or CO) can be formed. The study of CYP enzymatic reduction (the first electron transfer) demonstrated that both CPR and mitochondrial pair Adx/AdR could serve as an electron donor to micCYPs CYP2C9, CYP2C19, CYP1B1, CYP3A4, CYP3A5, CYP19A1, CYP21A2, CYP17A1 (Table 1). In this case, the effective transfer of the first electron does not always means the possibility of productive catalysis. Interestingly, microsomal steroidogenic CYP17A1, CYP21A2 and CYP19A1 were able to catalyze reactions using both CPR and the mitochondrial pair Adx/AdR as electron donors (Table 1). Other micCYPs did not show enzymatic activity with Adx/AdR. We found that CYP51A1 couldn't be reduced efficiently using

Table 1
Equilibrium dissociation constants (Kd) for CYPs/redox partners interactions and functional evaluation of CYPs.

Equilibrium dissociation constants (Kd), μM			First electron transfer		Catalytic activity		Substrate for catalytic activity assay
Cytochrome P450	Adx	CPR	Adx/AdR	CPR	Adx/AdR, min^{-1}	CPR, min^{-1}	
Microsomal CYPs							
CYP3A4	0.25 ± 0.01	1.50 ± 0,04	+	+	–	4.25 [36]	testosterone
CYP3A5	0.55 ± 0.03	0.70 ± 0.04	+	+	–	0.30	testosterone
CYP51	0.45 ± 0.03	0.30 ± 0.05	–	+	–	0.01 [25]	lanosterol
CYP2C9	0.70 ± 0.05	0.10 ± 0.02	+	+	–	5.25 [76]	diclofenac
CYP17A1	0.010 ± 0.003	1.80 ± 0.06	+	+	0.30	1.70 [34]	progesterone
CYP1B1	0.010 ± 0.003	0.020 ± 0,005	+	+	–	0.05 [37]	progesterone
CYP19A1	0.020 ± 0.001	0.11 ± 0.02	+	+	0.07	4.23 [34]	androstenedione
CYP21A2	0.10 ± 0.02	0.090 ± 0.002	+	+	39.6	18.60 [34]	progesterone
CYP2C19	0.030 ± 0.004	0.25 ± 0.03	+	+	–	4.70 [28]	omeprazole
Mitochondrial CYPs							
CYP11A1	0.010 ± 0.001	0.30 ± 0,02	+	–	3.26 [35]	–	7-dehydrocholesterol
CYP11B1	0.080 ± 0.004	0.30 ± 0.01	+	–	4.00 [35]	–	11-deoxycortisol
CYP11B2	0.040 ± 0.004	0.50 ± 0,03	+	–	2.76 [35]	–	11-deoxycortisol
Negative control							
CYP5A1	no	no	n/d	n/d	n/d	n/d	n/d

*"no" – complex formation was not observed ** "n/d" - not determined.

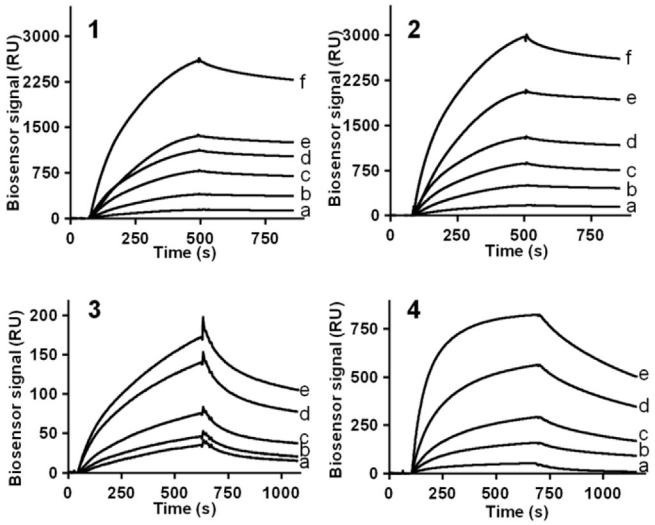

Fig. 1. SPR sensorgrams for micCYP (1–2) and mitCYP (3–4) interaction with immobilized CPR (1, 3) and Adx (2, 4) at 25 °C in HBS-EP + buffer. 1. CYP1B1/CPR a – 10 nM, b – 25 nM, c – 50 nM, d – 75 nM, e – 100 nM, f – 250 nM. 2. CYP1B1/Adx a – 10 nM, b – 25 nM, c – 50 nM, d – 75 nM, e – 100 nM, f – 250 nM. 3. CYP11A1/CPR a – 75 nM, b – 100 nM, c – 200 nM, d – 500 nM, e – 1000 nM 4. CYP11A1/Adx a – 10 nM, b – 30 nM, c – 50 nM, d – 75 nM, e – 100 nM.

the mitochondrial pair Adx/AdR (Fig. 2) while having almost equal affinity toward Adx and CPR (see Table 1).

It should be noted that positive results of complex formation between mitCYPs (CYP11A1, CYP11B1, CYP11B2) and CPR (Kd ~ 0.3–0.5 μM) were not accompanied by a productive electron transfer and catalytic activity using the standard CYP's substrates (Table 1), thereby demonstrating the functional selectivity of protein-protein interactions in the P450-dependent mitochondrial monooxygenase system.

3.2. Thermodynamic characterization of CYP/RP interactions by SPR

SPR analysis of CYP/RPs complex formation was performed at a temperature range from 10 to 40 °C, and sensorgrams are shown in Figs. 3.1–3.3 (as examples). The Van't Hoff plots were generated (Fig. 3.4) and thermodynamic parameters (ΔG, ΔH, -TΔS) of interaction between CYPs and their RPs were calculated (Table 2). All complexes of micCYPs/RPs and mitCYPs/PRs can be divided into three groups depending on the prevalent role of either enthalpy or entropy contribution. From Fig. 3.5 it follows that most complexes (about 90%) are entropy-driven, while the contribution of enthalpy and entropy differs significantly in the case of mitCYP/Adx complexes. The CYP11A1/Adx complex is enthalpy-driven, while CYP11B1/Adx and CYP11B2/Adx complexes are entropy-driven. The exception is the enthalpy/entropy-driven (mixed type) CYP21A2/Adx complex. Besides, there was no thermodynamic discrimination between the mitCYPs/CPR and micCYPs/CPR complexes (Table 2).

4. Discussion

4.1. Affinity and functional characterization of CYP/RP interactions by SPR

We have shown that the Kd values for the studied PPIs varied from 0.01 to 2 μM (Table 1) and this range is in accordance with the affinity data obtained for other CYP/CPR complexes: Kd ~ 0.2–0.3 μM for CYP2B4/CPR [19], Kd ~ 0,07 μM for CYP2B4/CPR and Kd ~ 0,1 μM for CYP2B1/CPR [7], Kd ~ 0.03–0.14 μM [38], and ~0,03 μM for CYP2C9/CYB5A [39]. It should be mentioned that the results obtained in this work are comparable with those from other studies describing the formation of P450 complex with RP and demonstrating the validity and reproducibility of the method used. The protein-protein interactions including those with RP are important for modulation of the CYP activity. Many studies have been performed in this field. It seems difficult to compare the parameters of the CYP-RP complex formation for many CYP isoforms because of different experimental conditions and methods used to study PPI. Also interactions of CYPs with RPs could be modulated by the presence of substrates and/or inhibitors, as well as by CYP/CYP interactions [8,40]. It should be noticed that Kd values for complexes of all three RPs (Adx, CPR, CYB5) with microsomal CYP3A4, CYP3A5, CYP51, CYP17A1 and all mitCYPs differed significantly and only for CYP1B1/Adx and CYP1B1/CYB5A [10] complexes Kd values (~0.01 μM) were identical.

It can be speculated that CYP51/CPR complex having Kd values comparable with other micCYP/CPR complexes (Table 1) but a rather low affinity (Kd ~ 70–10 μM) of CYP51 towards CYB5A (or CYB5B) [10] would mean that cytochrome b5 is not necessary for electron transfer in the CYP51 cycle. The study with purified CYP51

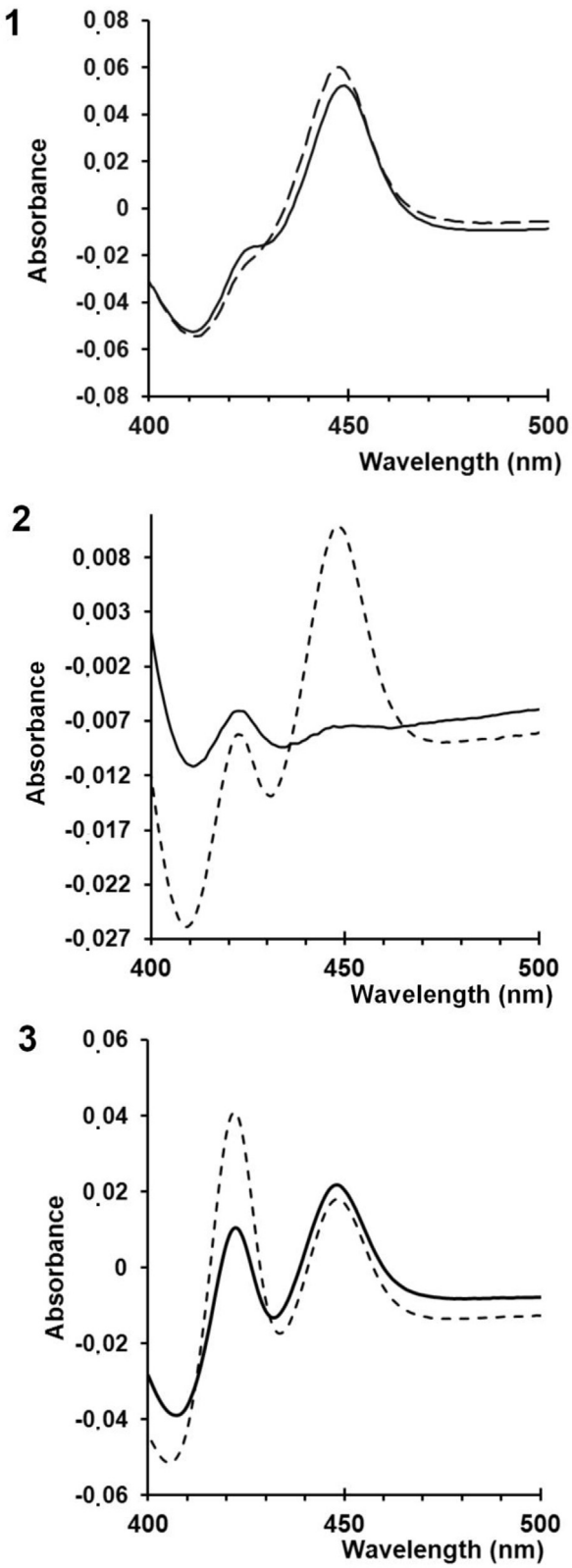

Fig. 2. Single-electron enzymatic reduction (solid line) of CYP51A1 (1 – with CPR, 2 – with Adx/AdR) and CYP17A1 (3 - with Adx/AdR). The dashed line represents a chemical reduction of CYP51A1 and CYP17A1 using sodium dithionite.

did not indicate on the CYP5A involvement in lanosterol demethylation [41]. However more recent work [42] has proven the ability of four different forms (coretail, the soluble core, signal-core, and the signal-coretail) of genetically engineered CYB5A to support the CYP51-mediated sterol 14α-demethylation reaction involving the hydroxylation and lyase activities. According to the dendrogram (Fig. 4.1), these results can also be due to the low similarity of CYP51 comparing with the other CYPs.

Otherwise, in our experiments, mitCYPs were able to receive the first electron only from the mitochondrial Adx/AdR pair and catalyzed the enzymatic reactions only in the presence of Adx/AdR (Table 1) indicating on high specificity towards Adx. Multiple sequence alignment of the mic- and mitCYPs (Fig. 4.3) revealed common features in the distribution of amino acids responsible for the interaction with electron donor proteins on the surface of micCYPs and mitCYPs [27,34]. The amino acids involved in the interaction with RP are located on the proximal surface of the protein which is opposite to the substrate-binding site (Figs. 4.2–4.3). Several overlaps are observed for the regions involved in the interaction with different electron-transfer proteins [6,34,35,43]. The ability of micCYP to interact with Adx is explained by the general structure of these regions, characteristic of all CYPs.

4.2. Entropy-driven complexes of micCYP/CPR

The formation of entropy-driven complexes micCYPs/CPRs (Table 2, Fig. 3.5) can be explained by the fact that a CPR molecule consists of two domains connected by a flexible linker, so it can exist in two conformations, “closed” and “open” [44]. When interacting with RPs (heme oxygenase and cytochrome c), the conformational transitions of CPR may occur from the “closed” to the “open” one [45,46]. The dynamic nature of interactions between CYPs and their electron transfer partners is hypothesized to be based on both a functional standpoint as well as a structural one [8]. Separate from its function as an electron transfer partner, CPR may also act as an allosteric effector to induce conformational changes in CYPs that modulate the rate of electron transfer. For bacterial CYP101, significant structural perturbations were observed by NMR upon complex formation with electron donor putidaredoxin [47,48]. Conformational plasticity may be one of the mechanisms by which the binding affinity of a CYP and its RP is modulated [49]. Thus, the CPR molecule undergoes significant structural rearrangements during the formation of the complex with CYP, which is associated with the negative value of -TΔS. The positive ΔH values of CYP/CPR complexes might be associated with the disruption of intramolecular hydrogen bonds and salt bridges occurring upon reductase conformational changes. In addition to conformational rearrangements, hydrophobic interactions between CYP and CPR membrane domains contribute to the entropy component ΔG [6,23,50]. In this work, we used truncated CYP19A1 and CYP21A2 lacking the membrane-anchoring domain. Therefore, it is possible that the hydrophobic domain of CPR interacts with other hydrophobic regions located on the CYP surface. The dissociation of complexes CYP/RPs (where RP means “redox partner”) was observed only in a high ionic strength solution containing detergents. Neither detergent nor high ionic strength separately caused the dissociation of CYP/RP complexes.

It should be noted that positive results of complex formation between mitCYPs (CYP11A1, CYP11B1, CYP11B2) and CPR (Kd ~ 0.3–0.5 μM) were not accompanied by a productive electron transfer and catalytic activity using the standard CYP's substrates (Table 1), thereby demonstrating the functional selectivity of protein-protein interactions in the P450 - dependent mitochondrial monooxygenase system. Besides, there was no thermodynamic discrimination between the mitCYPs/CPR and micCYPs/CPR complexes (Table 2).

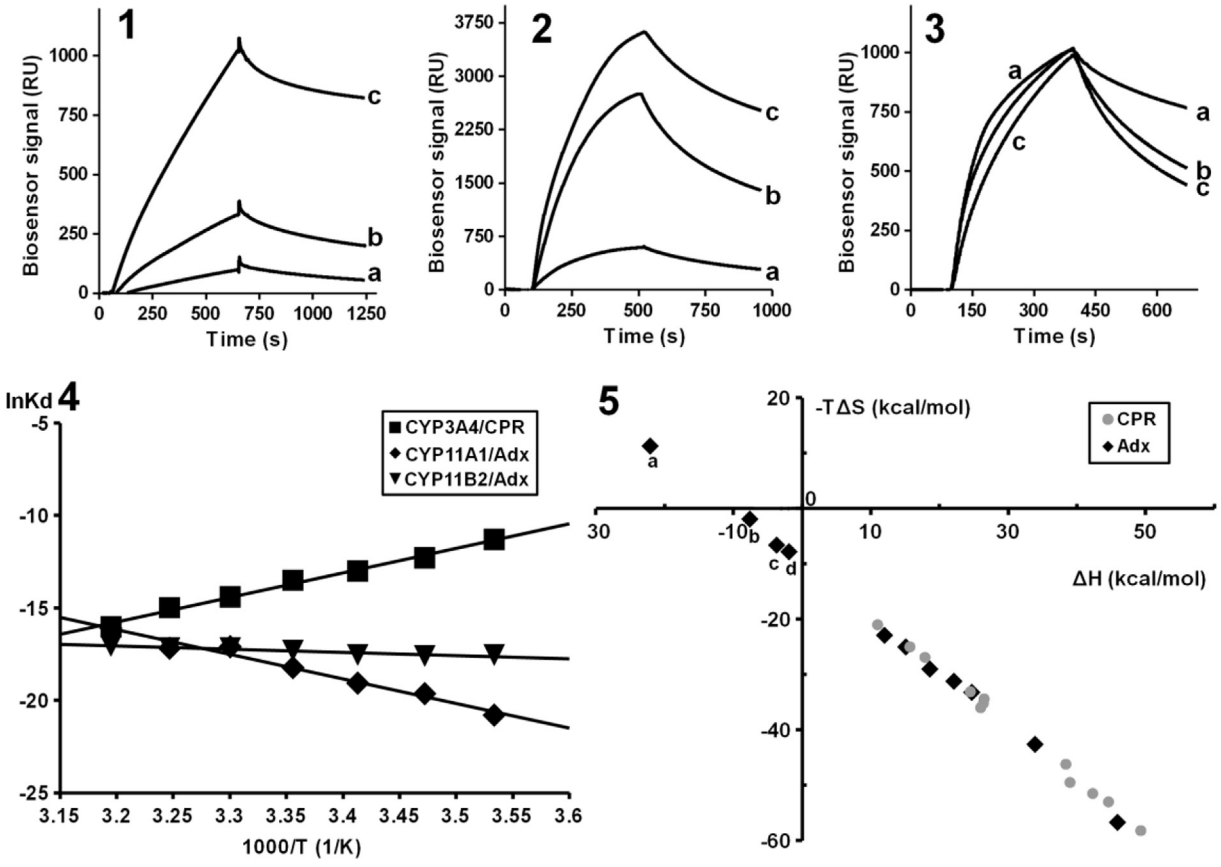

Fig. 3. Entropy-dependent, enthalpy-dependent, mixed PPI and calculation of their thermodynamic parameters. 1 – Sensorgrams of the entropy-driven interaction between immobilized CPR and CYP3A4 (1 μM) taken at different temperatures: a, b, and c – 10 °C, 25 °C, and 40 °C, respectively. 2 - Sensorgrams of the enthalpy-entropy-driven interaction between immobilized Adx and CYP11B2 (100 nM) taken at different temperatures: a, b, and c – 10 °C, 25 °C, and 40 °C, respectively. 3 - Sensorgrams of the enthalpy-driven interaction between immobilized Adx and CYP11A1 (100 nM) taken at different temperatures: a, b, and c – 10 °C, 25 °C, and 40 °C respectively. 4 – The van't Hoff plots for CYP3A4/CPR (squares), CYP11A1/Adx (rhombuses) and CYP11B2/Adx (triangles). 5 - Distribution of CYP/RP complexes into groups depending on the values of enthalpic (ΔH) and entropic (-TΔS) terms. CYP11A1/Adx – a, CYP21A2/Adx – b, CYP11B2/Adx – c, CYP11B1/Adx – d.

Table 2
Values of ΔG, ΔH and -TΔS for protein-protein complexes of cytochrome P450s with CPR and Adx.

Protein pair (analyte/ligand)	ΔG (kcal/mol)	ΔH (kcal/mol)	-TΔS (kcal/mol)
CYP3A4/CPR	−7.9 ± 0.2	27 ± 3	−34 ± 5
CYP3A5/CPR	−8.4 ± 0.2	45 ± 5	−53 ± 8
CYP51A1/CPR	−8.8 ± 0.7	26 ± 3	−35 ± 5
CYP17A1/CPR	−7.8 ± 0.3	38 ± 3	−46 ± 6
CYP2C9/CPR	−9.3 ± 0.5	42 ± 4	−51 ± 7
CYP2C19/CPR	9.0 ± 0.8	16 ± 2	−25 ± 3
CYP19A1/CPR	−9.5 ± 0.7	26 ± 3	−36 ± 4
CYP21A2/CPR	−9.6 ± 0.4	11 ± 1	−21 ± 2.
CYP1B1/CPR	−10.5 ± 0.9	39 ± 4	−49 ± 5
CYP11A1/CPR	−8.9 ± 0.8	49 ± 6	−58 ± 7
CYP11B2/CPR	−8.6 ± 0.4	24 ± 4	−33 ± 3
CYP11B1/CPR	−8.9 ± 0.3	18 ± 3	−27 ± 3
CYP3A4/Adx	−9.1 ± 0.3	22 ± 3	−31 ± 5
CYP3A5/Adx	−8.5 ± 0.4	25 ± 3	−33 ± 5
CYP51A1/Adx	−8.7 ± 0.3	34 ± 4	−43 ± 6
CYP17A1/Adx	−10.8 ± 0.9	12 ± 1	−23 ± 3
CYP2C9/Adx	−8.1 ± 0.5	48 ± 5	−56 ± 8
CYP2C19/Adx	−10.3 ± 2	18.6 ± 2	−29 ± 4
CYP19A1/Adx	−10.4 ± 1.2	15.1 ± 1.4	−25 ± 2
CYP21A2/Adx	−9.5 ± 0.8	−7.6 ± 0.6	−1.90 ± 0.02
CYP1B1/Adx	−10.8 ± 0.8	46 ± 5	−57 ± 6
CYP11A1/Adx	−10.8 ± 0.7	−22 ± 3	11 ± 1
CYP11B2/Adx	−10.3 ± 0.5	−3.7 ± 0.4	−6.6 ± 0.7
CYP11B1/Adx	−9.6 ± 0.4	−1.9 ± 0.2	−7.8 ± 0.8

Data represent mean ± SD of three independent experiments.

4.3. The entropy-driven complexes of micCYP/Adx

According to the data presented in Table 2 and Fig. 3.5, Adx forms the entropy-driven complexes with most micCYPs, excluding a mixed-type complex CYP21A2/Adx. The negative ΔH value of CYP21A2/Adx complex can be explained by the electrostatic interactions of the positively charged amino acids of CYP with the negatively charged amino acids of Adx. The negative -TΔS value of CYP21A2/Adx complex is probably due to the hydrophobic bonds formation. In general, the mechanism and the role of micCYP/Adx interactions are poorly described in the literature. Therefore, it is difficult to discuss the structural basis of the thermodynamic parameters obtained for those complexes formation. To summarize, no differentiation of the thermodynamic parameters was detected for the micCYP/RP complex formation.

4.4. Enthalpy-driven and mixed-type complexes of mitCYP/Adx

Enthalpy contribution to the mitCYP/Adx complex formation (Table 2 and Fig. 3.5) indicates that hydrogen and electrostatic bonds should be formed between interacting protein molecules. The crystal structure of CYP11A1/Adx complex is thoroughly described in Ref. [27] (Fig. 4.2). Briefly, it has been shown that the negatively charged amino acids of Adx (Asp72 and Asp76) form salt bridges with the positively charged amino acids (Lys339 and Lys343) of K-helix located on the surface of CYP11A1. The

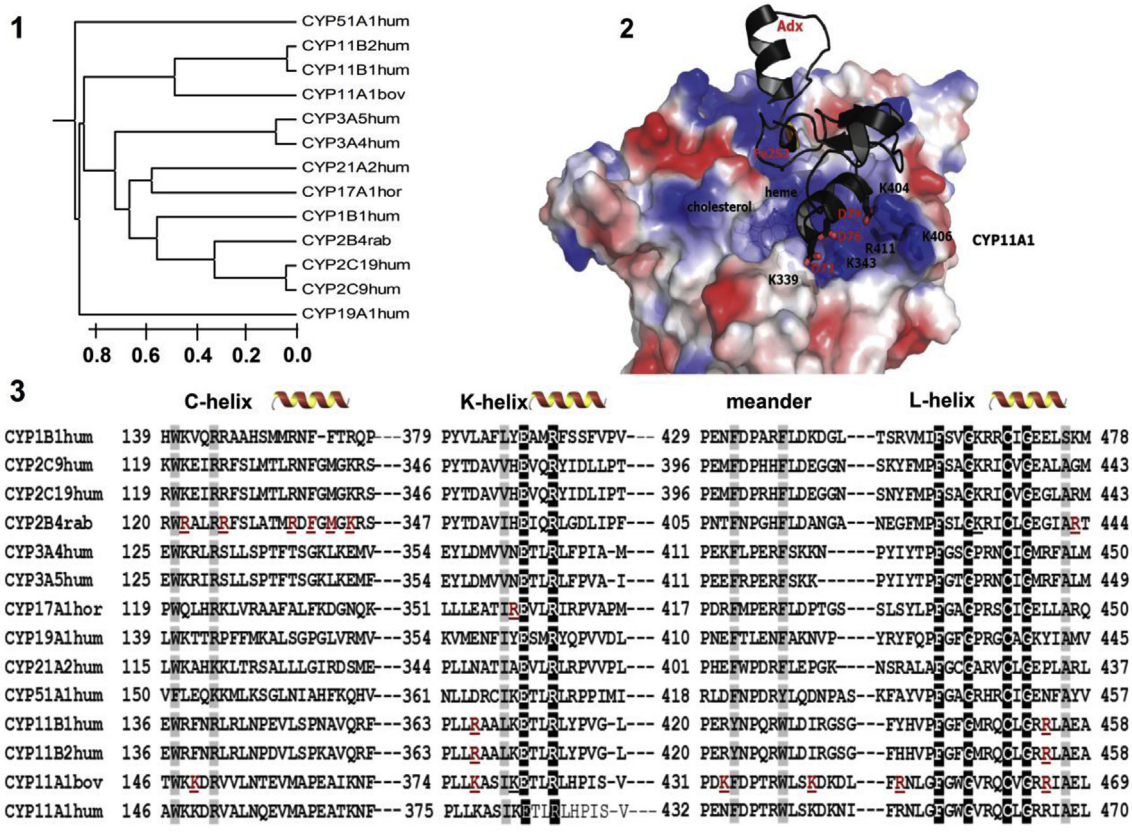

Fig. 4. The structural commonality of the CYPs under study and the principle of CYP/RP complex formation. **1.** The dendrogram shows CYPs studied in the present work. The genetic distance is marked horizontally. The evolutionary analysis was performed using the MEGA7 program [75]. **2.** Distribution of charged amino acid residues on the surface of human CYP11A1 and Adx [27]. Positively charged amino acids are highlighted in blue, negatively – in red. **3.** Multiple sequence alignment of the mic- and mitCYPs studied in the present work. The amino acids involved in the interaction with RP are underlined. We didn't use CYP2B4 in the current work; it is included in the alignment to demonstrate the amino acids involved in the interaction with redox partners [66]. hum- *Homo sapiens*; bov - *Bos taurus*, hor - *Equus caballus*, rab - *Oryctolagus cuniculus*.

importance of these electrostatic interactions has been previously experimentally confirmed [26,51,52]. It seems that the amino acid residue Asp79 of Adx affects the catalytic activity of CYP11A1 and interaction with the RPs, so this residue can interact with Lys404, Lys406 or Arg411 of CYP11A1 under conformational changes of the meander region (a loop on the proximal surface of the CYP molecule located close to the heme-binding region) [27]. For the CYP11B/Adx complexes, the negative ΔH and -TΔS values are typical, indicating the electrostatic and hydrophobic bonds formation. So far, there is no structural information available on the complexes of CYP11B1 and CYP11B2 with Adx. Nevertheless, multiple alignments of mitCYP sequences from different species [27,53] and an analysis of the crystal structure of CYP11B2 [35] reveal the charged amino acids Arg366, Lys370, Arg453, Lys357 of CYP11B1 and CYP11B2 involved in the interaction with Asp72, Asp76, and Asp79 of Adx [53]. The hydrophobic amino acids surrounding Asp80 of Adx could also play an important role in the interaction, which is in a good agreement with published data [54]. It was demonstrated that the substitution of Tyr82 of Adx with a more hydrophobic amino acid (Phe or Leu) resulted in a significant increase in the affinity of Adx to CYP11B1, but this mutation did not change the affinity to CYP11A1 [54]. The substitution of His56 of Adx with a more hydrophilic or polar amino acid (Thr, Gln, Arg) led to a more considerable change in the affinity of Adx to CYP11B1 comparing with the substitution of Asp76 [54]. The substitution of His56 and Tyr82 did not seriously affect the affinity of Adx to CYP11A1. Thus, we can conclude that the hydrophobic amino acids located between the iron-sulfur cluster and the region on the Adx surface containing negatively charged amino acids are crucial for the formation of the CYP11B1/Adx complex.

Based on the Kd values and the involvement of hydrophobic contacts in the interaction (-TΔS <0), the mitCYP/Adx complexes can be ranked as follows: CYP11B1> CYP11B2> CYP11A1 (Fig. 5.1). Interestingly, the difference in the -TΔS values for CYP11B1/Adx and CYP11B2/Adx complexes is not statistically significant, whereas the ΔH values for all mitCYP/Adx complexes differ markedly (Fig. 5.1). The following factors may influence either separately or simultaneously: a decrease in the number of electrostatic contacts and the formation of hydrophobic bonds to compensate for this decrease and/or the hydrophobic contacts preventing the occurrence of electrostatic bonds. To understand how the hydrophobic contacts affect Kd of mitCYP/Adx complexes, the association (k_{on}) and dissociation rate constants (k_{off}) of these complexes were analyzed (Fig. 5.2). It was shown that the k_{off} values were identical, while significant differences were recorded in the k_{on} values. Thus, CYP11A1/Adx is the most rapidly forming complex compared to other micCYPs/Adx complexes, while the CYP11B1/Adx complex has the lowest k_{on} value. This finding is consistent with the fact that CYP11A1 and CYP11B2 catalyze multistep reactions, whereas CYP11B1 catalyzes a one-step reaction. CYP11A1 catalyzes the key reaction in the biosynthesis of pregnenolone, which serves as a "raw material" for the production of steroid hormones. The high-affinity CYP11A1/Adx complex (Kd ~ 10 nM, see Table 1) provides a continuous supply of electrons for three-step oxidation of cholesterol to pregnenolone. Besides, higher k_{on} value of the CYP11A1/Adx compared to that of CYP11B/Adx reflects the priority

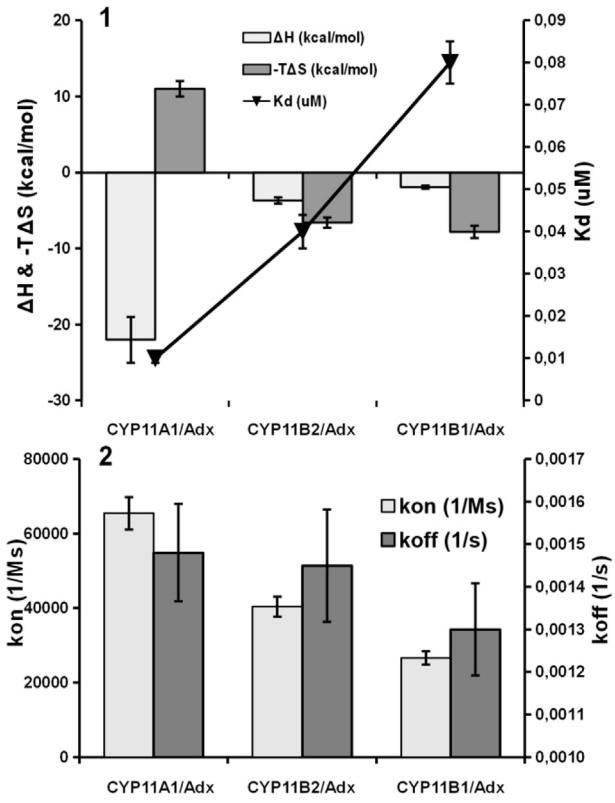

Fig. 5. The pattern characteristic of the mitCYP/Adx complex formation. 1. The mitCYP/Adx affinity reduction is consistent with the negative values of -TΔS and small absolute values of ΔH. While reducing the role of electrostatic interactions, the impact of hydrophobic contacts increases and the mitCYP/Adx complex becomes less stable. 2. The difference of dissociation rate constants (k_{off} values) of mitCYP/Adx complexes is not statistically significant, whereas the association rate consntants (k_{on} values) of complex formation differ significantly. The higher the Kd values, the less the k_{on} values.

of the usage of a common pool of mitochondrial Adx. It is possible that additional hydrophobic interactions may decrease the rate of CYP11B/Adx complex formation and therefore reduce the competition between CYP11B and CYP11A1 for Adx. However, the mechanism of this effect is unclear, because there is no data on the structure of CYP11B/Adx complex. The competition between CYP11B1 and CYP11B2 for Adx is not taking place since these proteins are localized in different zones of the adrenal cortex. The Kd values of CYP11B1/Adx and CYP11A1/Adx complexes are in accordance with data of other authors [55–57].

4.5. A specific functional way of steroidogenic microsomal CYPs

As for microsomal steroidogenic micCYPs, it was previously shown [34] that the first electron to truncated CYP17A1 may be supplied not only from CPR, but also a mitochondrial pair of electron donors support enzymatic reaction. In the present work, we have shown that the catalytic activity of a full-length CYP17A1 and CYP19A1 is considerably lower with Adx compared to CPR. However, CYP17A1/Adx and CYP19A1/Adx complexes have more than five times higher affinity compared to CYP17A1/CPR and CYP19A1/CPR (Table 1). Unexpectedly, the activity of CYP21A2 in the presence of Adx/AdR was 2-fold higher than in the presence of CPR, but the affinity of CYP21A2/CPR and CYP21A2/Adx complexes was not significantly differ (Table 1). This finding is consistent with the non-typical thermodynamics of the interaction between CYP21A2 and Adx which is similar to that for complex formation between CYP11B and Adx. Based on these results we suggested that there is a possibility of efficient electron transfer to CYP21A2 from ferredoxins. To test this hypothesis, we measured the activity of CYP21A1 in a reconstituted system with plant redox donor proteins (yeast Arh1 and ferredoxin 1 from spinach). We showed for the first time that different redox proteins, e.g., spinach ferredoxin could support the enzymatic activity of CYP21A2 (unpublished data).

Thus, CYP21A2 is a more universal electron acceptor than other micCYPs. This feature of CYP21A2 may be related to its key role in the biosynthesis of adrenal cortex hormones, which was also confirmed by the highest efficiency (k_{cat}/Km ratio) of the catalyzed reactions among mammalian CYPs [58]. Such high efficacy can also be the result of CYP21A2's convergent evolution aimed at increasing the number of RPs of this crucial enzyme since CYP21A1 deficiency is associated with severe clinical phenotypes [59]. However, the possibility that the mitochondrial electron donors support enzymatic reactions catalyzed by some micCYP has been reported earlier [34,60]. That phenomenon could be explained by the hypothesis assuming the origin of mitCYP from micCYP as proposed by Tsuneo Omura [61]. According to this hypothesis, CYPs are likely to diverge from a common ancestor gene, and therefore some of the CYPs may exhibit specificity with respect to different electron donor proteins. In other words, a significant similarity in the topology of regions involved in the interaction with redox partner provides the possibility of electron transfer and catalysis using different types of electron donors. Besides, the ability of mitochondrial pair Adx/AdR to support the catalytic activity of steroidogenic micCYP may be related to its crucial role in many biochemical pathways. Based on the observation that animals with a CPR gene knockout had the basal activity of several CYPs [62,63], it is likely that Adx/AdR could maintain the micCYP's activity *in vivo*. Also, patients with Antley-Bixler syndrome (CPR gene deficiency) were shown to have a basal CYPs activity [64]. CYP17A1 is a key enzyme of steroid hormone biosynthesis and also plays an important role in meiosis [65]. In contrast to drug-metabolizing CYPs, deficiency of this enzyme can be fatal for the organism.

We have also found that microsomal CYP/CPR complexes (including steroidogenic CYP17A1/CPR and CYP19A1/CPR) had slightly lower affinity compared to CYP/Adx, except for CYP2C9/CPR and CYP51/CPR complexes (Table 1). This fact most likely due to the adaptive universal role of CPR (less specific than Adx) in the electron transfer not only to micCYPs but to a number of proteins not belonging to the CYP superfamily: heme-oxygenase catalyzing the initial stages of heme biodegradation [66]; squalene monooxygenase participating in the synthesis of cholesterol [67]; CYB5A acting as an effector in a number of reactions catalyzed by micCYP and involved in the elongation of fatty acids [68].

4.6. Thermodynamic and functional characterization of CYP/RP complexes from evolutionary aspects of micCYPs and mitCYPs divergence

The P450-dependent electron transfer systems (ETS) can be categorized into ten classes [3] according to the topology and cellular localization of the protein components involved in electron transfer to CYPs. The main classes are ETS-1 (mitochondrial CYPs acquire electrons from Adx/AdR) and ETS-2 (microsomal CYPs acquire electrons from CPR). ETS-2 and ETS-1 evolved from a common ancestor [69]. In the present work, we have demonstrated that the intermolecular recognition between RP and mit-, micCYPs differs significantly and some characteristic features of the divergence of ETS-1 and ETS-2 should be highlighted:

(i) During the evolution mitCYPs underwent significant changes in the electron transport system increasing their specificity for RP. Such changes could be explained by the existence of

many other ETSs in mitochondria [70]. High specificity of mitCYP to RP prevents the "unauthorized" transfer of electrons from non-monooxygenase ETSs. This specificity could result from the structural rearrangement of mitCYP during the interaction with Adx (but not with CPR).

(ii) The versatility of ETS-2 may be necessary since dozens of micCYPs with different functional roles, catalyzing numerous chemical reactions and possessing wide substrate specificity, receive electrons from CPR as a single "supplier". Perhaps, this feature prevents the differentiation of micCYP/RP interactions. Therefore, the regulation of ETS-2 activity involves alternative electron acceptors [8], of which CYB5A is the most known. This hemoprotein is capable of modulating the activity of some micCYPs [36,71]. A CYP/CYP interaction is another mechanism of regulation [31,72,73]. Also, micCYPs can interact with other proteins, for example, the receptor of progesterone PGRMC1 [71]. Therefore, a large number of factors ensuring the versatility of ETS-2 ultimately contribute to the overall adaptation of an organism to the constantly changing environmental conditions.

(iii) A high degree of mitCYP specialization may be associated with their narrow substrate specificity. In the present study, we observed a specific correlation between the changes in the entropy component (-TΔS) and k_{on} for mitCYP/Adx complexes. The rate of electron transfer depends on the rate of CYP/RP complex formation. Thus, the mechanism of electron transfer to mitCYP can be considered as a regulating factor in the overall catalysis performed by mitCYPs.

To summarize, from the evolution point of view, the specialization of PPIs, accompanied by an increase in the specificity of electron transfer significantly increased for ETS-1. Unlike ETS-1, the evolution of ETS-2 leads to an increase in versatility as demonstrated for steroidogenic microsomal CYP17A1, CYP19A1, and CYP21A2.

5. Conclusion

A large-scale comparative study of the affinity and thermodynamic parameters of interactions of 12 different cytochrome CYPs (20% of all known human CYPs from 9 out of 18 families [74]) and their RP (Adx, CPR) has been performed. We have observed thermodynamic discrimination for interactions of mitCYPs with Adx associated with the different functional impact of CYP11A1 and CYP11B. Besides, the formation of mitCYP/Adx complex was regulated by changing the association rate constant. The main driving force in the formation of CYP/Adx and CYP/CPR complexes is the entropy contribution, which may be critical for productive electron transfer. We have also shown that there is a differentiation of enthalpy-driven complexes depending on CYP's redox partner. For example, in the present study CYP11A1/Adx complex was only enthalpy-driven, CYP21A2 - enthalpy/entropy-driven (mixed type). From the evolutionary point of view, mitCYPs significantly increased the specialization of PPIs, which was accompanied by an increase in the specificity of electron transfer. Unlike mitCYPs, the evolution of micCYPs leads to an increase in versatility as demonstrated for steroidogenic CYP17A1, CYP19A1, and CYP21A2.

Author contributions

Y.E.O. and F.A.V. performed all biosensor experiments and calculated the thermodynamic parameters of protein-protein interactions. S.T.V. and G.I.P. performed spectral and biochemical studies of CYP/RP interactions. S.T.A., G.A.A., Y.E.O., E.P.V. and S.N.V. formulated the main idea and developed the text of the article. G.A.A., E.P.V., G.O.V., L.A.K., U.S.A., I.A.S. designed the project, supervised the data analysis and critically revised the manuscript.

Funding

The work was done within the framework of the State Academies of Sciences Fundamental Scientifc Research Program for 2013–2020 and partly supported by the Russian Foundation for Basic Research (project No 18-04-00071) (SPR analysis of interactions between CYP21A2, CYP17A1, CYP2C19 and redox partners and CYP's substrates). SPR measurements were performed using the equipment of "Human Proteome" Core Facilities of the Institute of Biomedical Chemistry (Russia).

Declaration of interests

The authors declare that they have no known competing financial interests or personal relationships that could have appeared to influence the work reported in this paper.

Acknowledgments

We thank Dr. Smolskaya S.V. and Svirid A.V., Luschik A.Y., Tumilovich A.M., Haidukevich I.V. from the Institute of Bioorganic Chemistry for providing support in CYP protein purification.

References

[1] F.P. Guengerich, Z.-L. Wu, C.J. Bartleson, Function of human cytochrome P450s: characterization of the orphans, Biochem. Biophys. Res. Commun. 338 (2005) 465–469, https://doi.org/10.1016/j.bbrc.2005.08.079.

[2] U.M. Zanger, M. Schwab, Cytochrome P450 enzymes in drug metabolism: regulation of gene expression, enzyme activities, and impact of genetic variation, Pharmacol. Therapeut. 138 (2013) 103–141, https://doi.org/10.1016/j.pharmthera.2012.12.007.

[3] F. Hannemann, A. Bichet, K.M. Ewen, R. Bernhardt, Cytochrome P450 systems—biological variations of electron transport chains, Biochim. Biophys. Acta Gen. Subj. 1770 (2007) 330–344, https://doi.org/10.1016/j.bbagen.2006.07.017.

[4] A. Wada, M.R. Waterman, Identification by site-directed mutagenesis of two lysine residues in cholesterol side chain cleavage cytochrome P450 that are essential for adrenodoxin binding, J. Biol. Chem. 267 (1992) 22877–22882.

[5] A.V. Pandey, C.E. Flück, NADPH P450 oxidoreductase: structure, function, and pathology of diseases, Pharmacol. Therapeut. 138 (2013) 229–254, https://doi.org/10.1016/j.pharmthera.2013.01.010.

[6] P. Hlavica, J. Schulze, D.F.V. Lewis, Functional interaction of cytochrome P450 with its redox partners: a critical assessment and update of the topology of predicted contact regions, J. Inorg. Biochem. 96 (2003) 279–297, https://doi.org/10.1016/S0162-0134(03)00152-1.

[7] D.F.V. Lewis, P. Hlavica, Interactions between redox partners in various cytochrome P450 systems: functional and structural aspects, Biochim. Biophys. Acta Bioenerg. 1460 (2000) 353–374, https://doi.org/10.1016/S0005-2728(00)00202-4.

[8] S.E. Kandel, J.N. Lampe, Role of protein–protein interactions in cytochrome P450-mediated drug metabolism and toxicity, Chem. Res. Toxicol. 27 (2014) 1474–1486, https://doi.org/10.1021/tx500203s.

[9] A.V. Veselovsky, Y.D. Ivanov, A.S. Ivanov, A.I. Archakov, P. Lewi, P. Janssen, Protein–protein interactions: mechanisms and modification by drugs, J. Mol. Recognit. 15 (2002) 405–422, https://doi.org/10.1002/jmr.597.

[10] E. Yablokov, A. Florinskaya, A. Medvedev, G. Sergeev, N. Strushkevich, A. Luschik, T. Shkel, I. Haidukevich, A. Gilep, S. Usanov, A. Ivanov, Thermodynamics of interactions between mammalian cytochromes P450 and b5, Arch. Biochem. Biophys. 619 (2017) 10–15, https://doi.org/10.1016/j.abb.2017.02.006.

[11] K. Retra, H. Irth, J.E. van Muijlwijk-Koezen, Surface Plasmon Resonance biosensor analysis as a useful tool in FBDD, Drug Discov. Today Technol. 7 (2010) e181–e187, https://doi.org/10.1016/j.ddtec.2010.11.012.

[12] N.J. de Mol, F.J. Dekker, I. Broutin, M.J.E. Fischer, R.M.J. Liskamp, Surface plasmon resonance thermodynamic and kinetic analysis as a strategic tool in drug design. Distinct ways for phosphopeptides to plug into src- and Grb2 SH2 domains, J. Med. Chem. 48 (2005) 753–763, https://doi.org/10.1021/jm049359e.

[13] B.K. Kaiser, F. Barahmand-pour, W. Paulsene, S. Medley, D.E. Geraghty, R.K. Strong, Interactions between NKG2x immunoreceptors and HLA-E ligands display overlapping affinities and thermodynamics, J. Immunol. 174 (2005) 2878–2884, https://doi.org/10.4049/jimmunol.174.5.2878.

[14] R.F. Kelley, Thermodynamics of protein-protein interaction studied by using BIAcore and single-site mutagenesis, Methods 6 (1994) 111–120, https://doi.org/10.1006/meth.1994.1014.
[15] H. Roos, R. Karlsson, H. Nilshans, A. Persson, Thermodynamic analysis of protein interactions with biosensor technology, J. Mol. Recognit. 11 (1998) 204–210, https://doi.org/10.1002/(SICI)1099-1352(199812)11:1/6<204::AID-JMR424>3.0.CO;2-T.
[16] J.M. McDonnell, Surface plasmon resonance: towards an understanding of the mechanisms of biological molecular recognition, Curr. Opin. Chem. Biol. 5 (2001) 572–577, https://doi.org/10.1016/S1367-5931(00)00251-9.
[17] J.N. Lampe, Advances in the understanding of protein-protein interactions in drug metabolizing enzymes through the use of biophysical techniques, Front. Pharmacol. 8 (2017), https://doi.org/10.3389/fphar.2017.00521.
[18] J.T. Pearson, J.J. Hill, J. Swank, N. Isoherranen, K.L. Kunze, W.M. Atkins, Surface plasmon resonance analysis of antifungal azoles binding to CYP3A4 with kinetic resolution of multiple binding orientations, Biochemistry 45 (2006) 6341–6353, https://doi.org/10.1021/bi0600042.
[19] Y.D. Ivanov, I.P. Kanaeva, M.A. Eldarov, K.G. Sklyabin, M. Lehnerer, J. Schulze, P. Hlavica, A.I. Archakov, An optical biosensor study of the interaction parameters and role of hydrophobic tails of cytochrome P450 2B4, b5 and NADPH-flavoprotein in complex formation, IUBMB Life 42 (1997) 731–737, https://doi.org/10.1080/15216549700203161.
[20] Y.D. Ivanov, I.P. Kanaeva, V.Y. Kuznetsov, M. Lehnerer, J. Schulze, P. Hlavica, A.I. Archakov, The optical biosensor studies on the role of hydrophobic tails of NADPH-cytochrome P450 reductase and cytochromes P450 2B4 and b5 upon productive complex formation within a monomeric reconstituted system, Arch. Biochem. Biophys. 362 (1999) 87–93, https://doi.org/10.1006/abbi.1998.0981.
[21] Y.D. Ivanov, I.P. Kanaeva, I.I. Karuzina, S.A. Usanov, G. Hui Bon Hoa, S.G. Sligar, A.I. Archakov, Revelation of ternary complexes between redox partners in cytochrome P450-containing monooxygenase systems by the optical biosensor method, J. Inorg. Biochem. 87 (2001) 175–184, https://doi.org/10.1016/S0162-0134(01)00332-4.
[22] A.I. Archakov, Y.D. Ivanov, Application of AFM and optical biosensor for investigation of complexes formed in P450-containing monooxygenase systems, Biochim. Biophys. Acta Protein Proteonomics 1814 (2011) 102–110, https://doi.org/10.1016/j.bbapap.2010.08.013.
[23] A.A. Gilep, O.L. Guryev, S.A. Usanov, R.W. Estabrook, Apo-cytochrome b5 as an indicator of changes in heme accessability:: preliminary studies with cytochrome P450 3A4, J. Inorg. Biochem. 87 (2001) 237–244, https://doi.org/10.1016/S0162-0134(01)00333-6.
[24] A.A. Gilep, R.W. Estabrook, S.A. Usanov, Molecular cloning and heterologous expression in E. coli of cytochrome P45017α. Comparison of structural and functional properties of substrate-specific cytochromes P450 from different species, Biochemistry (Mosc.) 68 (2003) 86–98, https://doi.org/10.1023/A:1022101703670.
[25] N. Strushkevich, S.A. Usanov, H.-W. Park, Structural basis of human CYP51 inhibition by antifungal azoles, J. Mol. Biol. 397 (2010) 1067–1078, https://doi.org/10.1016/j.jmb.2010.01.075.
[26] S.A. Usanov, S.E. Graham, G.I. Lepesheva, T.N. Azeva, N.V. Strushkevich, A.A. Gilep, R.W. Estabrook, J.A. Peterson, Probing the interaction of bovine cytochrome P450scc (CYP11A1) with Adrenodoxin: evaluating site-directed mutations by molecular modeling, Biochemistry 41 (2002) 8310–8320, https://doi.org/10.1021/bi0255928.
[27] N. Strushkevich, F. MacKenzie, T. Cherkesova, I. Grabovec, S. Usanov, H.-W. Park, Structural basis for pregnenolone biosynthesis by the mitochondrial monooxygenase system, Proc. Natl. Acad. Sci. Unit. States Am. 108 (2011) 10139–10143, https://doi.org/10.1073/pnas.1019441108.
[28] I.V. Haidukevich, A.A. Gilep, T.S. Cherkesova, S.A. Usanov, Cloning, heterologous expression, isolation and purification of the human cytochrome CYP2C9 * 1, CYP2C9 * 2 and CYP2C9 * proteins, Proc. Nat. Acad. Sci. Belarus. Series Chem. Sci. 3 (2012) 105–111.
[29] Y. Sagara, T. Hara, Y. Ariyasu, F. Ando, N. Tokunaga, T. Horiuchi, Direct expression in Escherichia coli and characterization of bovine adrenodoxins with modified amino-terminal regions, FEBS (Fed. Eur. Biochem. Soc.) Lett. 300 (1992) 208–212, https://doi.org/10.1016/0014-5793(92)80847-A.
[30] Y. Sagara, A. Wada, Y. Takata, M.R. Waterman, K. Sekimizu, T. Horiuchi, Direct expression of adrenodoxin reductase in Escherichia coli and the functional characterization, Biol. Pharm. Bull. 16 (1993) 627–630, https://doi.org/10.1248/bpb.16.627.
[31] A.V. Svirid, P.V. Ershov, E.O. Yablokov, L.A. Kaluzhskiy, Y.V. Mezentsev, A.V. Florinskaya, T.A. Sushko, N.V. Strushkevich, A.A. Gilep, S.A. Usanov, A.E. Medvedev, A.S. Ivanov, Direct molecular fishing of new protein partners for human thromboxane synthase, Acta Naturae 9 (2017) 92–100.
[32] N. Romero, R. Radi, E. Linares, O. Augusto, C.D. Detweiler, R.P. Mason, A. Denicola, Reaction of human hemoglobin with peroxynitrite isomerization to nitrate and secondary formation of protein radicals, J. Biol. Chem. 278 (2003) 44049–44057, https://doi.org/10.1074/jbc.M305895200.
[33] T. Omura, R. Sato, The carbon monoxide-binding pigment of liver microsomes I. Evidence for its hemoprotein nature, J. Biol. Chem. 239 (1964) 2370–2378.
[34] T.A. Pechurskaya, I.N. Harnastai, I.P. Grabovec, A.A. Gilep, S.A. Usanov, Adrenodoxin supports reactions catalyzed by microsomal steroidogenic cytochrome P450s, Biochem. Biophys. Res. Commun. 353 (2007) 598–604, https://doi.org/10.1016/j.bbrc.2006.12.047.
[35] N. Strushkevich, A.A. Gilep, L. Shen, C.H. Arrowsmith, A.M. Edwards, S.A. Usanov, H.-W. Park, Structural insights into aldosterone synthase substrate specificity and targeted inhibition, Mol. Endocrinol. 27 (2013) 315–324, https://doi.org/10.1210/me.2012-1287.
[36] G.V. Sergeev, A.A. Gilep, S.A. Usanov, The role of cytochrome b5 structural domains in interaction with cytochromes P450, Biochemistry Moscow 79 (2014) 406–416, https://doi.org/10.1134/S0006297914050046.
[37] A.E. Luschik, A.A. Gilep, S.A. Usanov, Heterologous expression, isolation, purification and physical-chemical characterization of recombinant human CYP1B1, in: The Proceedings of the National Academy of Sciences of Belarus. Series of Chemical Sciences, 1, 2015, pp. 79–84.
[38] C. Barnaba, E. Taylor, J.A. Brozik, Dissociation constants of cytochrome P450 2C9/cytochrome P450 reductase complexes in a lipid bilayer membrane depend on NADPH: a single-protein tracking study, J. Am. Chem. Soc. 139 (2017) 17923–17934, https://doi.org/10.1021/jacs.7b08750.
[39] C.W. Locuson, L.C. Wienkers, J.P. Jones, T.S. Tracy, CYP2C9 protein interactions with cytochrome b5: effects on the coupling of catalysis, Drug Metab. Dispos. 35 (2007) 1174–1181, https://doi.org/10.1124/dmd.107.014910.
[40] T. Shimada, R.L. Mernaugh, F.P. Guengerich, Interactions of mammalian cytochrome P450, NADPH-cytochrome P450 reductase, and cytochrome b5 enzymes, Arch. Biochem. Biophys. 435 (2005) 207–216, https://doi.org/10.1016/j.abb.2004.12.008.
[41] J. Trzaskos, S. Kawata, J.L. Gaylor, Microsomal enzymes of cholesterol biosynthesis. Purification of lanosterol 14 alpha-methyl demethylase cytochrome P-450 from hepatic microsomes, J. Biol. Chem. 261 (1986) 14651–14657.
[42] D.C. Lamb, N.N. Kaderbhai, K. Venkateswarlu, D.E. Kelly, S.L. Kelly, M.A. Kaderbhai, Human sterol 14α-demethylase activity is enhanced by the membrane-bound state of cytochrome b5, Arch. Biochem. Biophys. 395 (2001) 78–84, https://doi.org/10.1006/abbi.2001.2566.
[43] A. Bridges, L. Gruenke, Y.-T. Chang, I.A. Vakser, G. Loew, L. Waskell, Identification of the binding site on cytochrome P450 2B4 for cytochrome b 5 and cytochrome P450 reductase, J. Biol. Chem. 273 (1998) 17036–17049, https://doi.org/10.1074/jbc.273.27.17036.
[44] J. Ellis, A. Gutierrez, I.L. Barsukov, W.-C. Huang, J.G. Grossmann, G.C.K. Roberts, Domain motion in cytochrome P450 reductase conformational equilibria revealed BY NMR and SMALL-ANGLE X-RAY scattering, J. Biol. Chem. 284 (2009) 36628–36637, https://doi.org/10.1074/jbc.M109.054304.
[45] M. Sugishima, H. Sato, Y. Higashimoto, J. Harada, K. Wada, K. Fukuyama, M. Noguchi, Structural basis for the electron transfer from an open form of NADPH-cytochrome P450 oxidoreductase to heme oxygenase, Proc. Natl. Acad. Sci. Unit. States Am. 111 (2014) 2524–2529, https://doi.org/10.1073/pnas.1322034111.
[46] S.L. Freeman, A. Martel, J.M. Devos, J. Basran, E.L. Raven, G.C.K. Roberts, Solution structure of the cytochrome P450 reductase–cytochrome c complex determined by neutron scattering, J. Biol. Chem. 293 (2018) 5210–5219, https://doi.org/10.1074/jbc.RA118.001941.
[47] B. OuYang, S.S. Pochapsky, M. Dang, T.C. Pochapsky, A functional proline switch in cytochrome P450cam, Structure 16 (2008) 916–923, https://doi.org/10.1016/j.str.2008.03.011.
[48] Y. Hiruma, M.A.S. Hass, Y. Kikui, W.-M. Liu, B. Ölmez, S.P. Skinner, A. Blok, A. Kloosterman, H. Koteishi, F. Löhr, H. Schwalbe, M. Nojiri, M. Ubbink, The structure of the cytochrome P450cam–putidaredoxin complex determined by paramagnetic NMR spectroscopy and crystallography, J. Mol. Biol. 425 (2013) 4353–4365, https://doi.org/10.1016/j.jmb.2013.07.006.
[49] S.S. Pochapsky, M. Dang, B. OuYang, A.K. Simorellis, T.C. Pochapsky, Redox-dependent dynamics in cytochrome P450cam, Biochemistry 48 (2009) 4254–4261, https://doi.org/10.1021/bi900002k.
[50] M.-S. Dong, H. Yamazaki, Z. Guo, F.P. Guengerich, Recombinant human cytochrome P450 1A2 and an N-Terminal-Truncated form: construction, purification, aggregation properties, and interactions with flavodoxin, ferredoxin, and NADPH-cytochrome P450 reductase, Arch. Biochem. Biophys. 327 (1996) 11–19, https://doi.org/10.1006/abbi.1996.0086.
[51] V.M. Coghlan, L.E. Vickery, Site-specific mutations in human ferredoxin that affect binding to ferredoxin reductase and cytochrome P450scc, J. Biol. Chem. 266 (1991) 18606–18612.
[52] V.M. Coghlan, L.E. Vickery, Electrostatic interactions stabilizing ferredoxin electron transfer complexes. Disruption by “conservative” mutations, J. Biol. Chem. 267 (1992) 8932–8935.
[53] H.-M. Peng, R.J. Auchus, Molecular recognition in mitochondrial cytochromes P450 that catalyze the terminal steps of corticosteroid biosynthesis, Biochemistry 56 (2017) 2282–2293, https://doi.org/10.1021/acs.biochem.7b00034.
[54] V. Beckert, R. Bernhardt, Specific aspects of electron transfer from adrenodoxin to cytochromes P450scc and P45011β, J. Biol. Chem. 272 (1997) 4883–4888, https://doi.org/10.1074/jbc.272.8.4883.
[55] B. Schiffler, A. Zöllner, R. Bernhardt, Stripping down the mitochondrial cholesterol hydroxylase system, a kinetics study, J. Biol. Chem. 279 (2004) 34269–34276, https://doi.org/10.1074/jbc.M402798200.
[56] A. Zöllner, M.A. Pasquinelli, R. Bernhardt, D.N. Beratan, Protein phosphorylation and intermolecular electron transfer: a joint experimental and computational study of a hormone biosynthesis pathway, J. Am. Chem. Soc. 129 (2007) 4206–4216, https://doi.org/10.1021/ja064803j.
[57] A. Zöllner, N. Kagawa, M.R. Waterman, Y. Nonaka, K. Takio, Y. Shiro, F. Hannemann, R. Bernhardt, Purification and functional characterization of human 11beta hydroxylase expressed in Escherichia coli, FEBS J. 275 (2008)

799–810, https://doi.org/10.1111/j.1742-4658.2008.06253.x.
[58] P.S. Pallan, C. Wang, L. Lei, F.K. Yoshimoto, R.J. Auchus, M.R. Waterman, F.P. Guengerich, M. Egli, Human cytochrome P450 21A2, the major steroid 21-hydroxylase structure OF the ENZYME·PROGESTERONE substrate complex and RATE-LIMITING C–H bond cleavage, J. Biol. Chem. 290 (2015) 13128–13143, https://doi.org/10.1074/jbc.M115.646307.
[59] P.C. White, P.W. Speiser, Congenital adrenal hyperplasia due to 21-hydroxylase deficiency, Endocr. Rev. 21 (2000) 245–291, https://doi.org/10.1210/edrv.21.3.0398.
[60] H.K. Anandatheerthavarada, S. Addya, J. Mullick, N.G. Avadhani, Interaction of adrenodoxin with P4501A1 and its truncated form P450MT2 through different Domains: differential modulation of enzyme activities, Biochemistry 37 (1998) 1150–1160, https://doi.org/10.1021/bi972046j.
[61] T. Omura, O. Gotoh, Evolutionary origin of mitochondrial cytochrome P450, J. Biochem. 161 (2017) 399–407, https://doi.org/10.1093/jb/mvx011.
[62] J. Gu, Y. Weng, Q.-Y. Zhang, H. Cui, M. Behr, L. Wu, W. Yang, L. Zhang, X. Ding, Liver-specific deletion of the NADPH-cytochrome P450 reductase gene impact ON plasma cholesterol homeostasis and the function and regulation OF microsomal cytochrome P450 and heme oxygenase, J. Biol. Chem. 278 (2003) 25895–25901, https://doi.org/10.1074/jbc.M303125200.
[63] B.B. Dunning, X. Machne, Membrane capacitance measurements during acetylcholine action, Neuropharmacology 15 (1976) 73–75, https://doi.org/10.1016/0028-3908(76)90100-3.
[64] C.E. Flück, W.L. Miller, P450 oxidoreductase deficiency: a new form of congenital adrenal hyperplasia, Curr. Opin. Pediatr. 18 (2006) 435–441, https://doi.org/10.1097/01.mop.0000236395.71956.5c.
[65] A.A. Gilep, T.A. Sushko, S.A. Usanov, At the crossroads of steroid hormone biosynthesis: the role, substrate specificity and evolutionary development of CYP17, Biochim. Biophys. Acta Protein Proteonomics 1814 (2011) 200–209, https://doi.org/10.1016/j.bbapap.2010.06.021.
[66] B.A. Schacter, E.B. Nelson, H.S. Marver, B.S.S. Masters, Immunochemical evidence for an association of heme oxygenase with the microsomal electron transport system, J. Biol. Chem. 247 (1972) 3601–3607.
[67] O. Teruo, O. Shigeru, H. Fumihiko, I. Yoh, Involvement of NADPH-cytochrome c reductase in the rat liver squalene epoxidase system, Biochim. Biophys. Acta Lipids Lipid Metab. 486 (1977) 401–407, https://doi.org/10.1016/0005-2760(77)90089-3.
[68] H.G. Enoch, P. Strittmatter, Cytochrome b5 reduction by NADPH-cytochrome P-450 reductase, J. Biol. Chem. 254 (1979) 8976–8981.
[69] D.F.V. Lewis, G. Sheridan, Cytochromes P450, oxygen, and evolution, Sci. World J. (2001), https://doi.org/10.1100/tsw.2001.22.
[70] J.A. Enríquez, Supramolecular organization of respiratory complexes, Annu. Rev. Physiol. 78 (2016) 533–561, https://doi.org/10.1146/annurev-physiol-021115-105031.
[71] T.D. Porter, The roles of cytochrome b5 in cytochrome P450 reactions, J. Biochem. Mol. Toxicol. 16 (2002) 311–316, https://doi.org/10.1002/jbt.10052.
[72] T.A. Sushko, A.A. Gilep, S.A. Usanov, Mechanism of intermolecular interactions of microsomal cytochrome P450s CYP17 and CYP21 involved in steroid hormone biosynthesis, Biochemistry Moscow 77 (2012) 585–592, https://doi.org/10.1134/S0006297912060041.
[73] D.R. Davydov, N.Y. Davydova, E.V. Sineva, J.R. Halpert, Interactions among cytochromes P450 in microsomal membranes oligomerization OF cytochromes P450 3A4, 3A5, and 2E1 and its functional consequences, J. Biol. Chem. 290 (2015) 3850–3864, https://doi.org/10.1074/jbc.M114.615443.
[74] W. Nebert Daniel, Wikvall Kjell, L. Miller Walter, Human cytochromes P450 in health and disease, Phil. Trans. Biol. Sci. 368 (2013) 20120431, https://doi.org/10.1098/rstb.2012.0431.
[75] S. Kumar, G. Stecher, K. Tamura, MEGA7: molecular evolutionary genetics analysis version 7.0 for bigger datasets, Mol. Biol. Evol. 33 (2016) 1870–1874, https://doi.org/10.1093/molbev/msw054.
[76] I.V. Haidukevich, T.A. Sushko, A.M. Tumilovich, I.P. Grabovec, S.A. Usanov, A.A. Gilep, Different inhibitory effects of azole-containing drugs and pesticides on CYP2C9 polymorphic forms: an in vitro study, Toxicol. Vitro 50 (2018) 249–256, https://doi.org/10.1016/j.tiv.2018.04.002.